MODEL DEVELOPMENT FOR BROAD AREA EVENT IDENTIFICATION AND YIELD ESTIMATION

W. Scott Phillips[1], Xiaoning Yang[1], Richard J. Stead[1], Michael L. Begnaud[1], and Kevin M. Mayeda[2]

Los Alamos National Laboratory[1] and Weston Geophysical[2]

Sponsored by the National Nuclear Security Administration

Award Number: DE-AC52-06NA25396/LA10-Yield-NDD02

ABSTRACT

Models of laterally varying attenuation and site effects of regional phases are necessary to correct regional phase and coda amplitudes to reveal source effects of importance to identification and yield estimation procedures. We accomplish this using 2-D amplitude tomography, incorporating ground truth spectral estimates based on relative coda techniques and regional moment tensor inversion. The ground truth spectra allow calibration to absolute levels, and can be used to validate amplitude prediction models. Ground truth spectra may also be used to improve resolution in the margins of raypath coverage where source-path tradeoffs would otherwise dominate. Initial studies using USArray amplitude data show that we can recover frequency dependent, laterally varying attenuation, absolute site terms, moment and apparent stress using constraints based on ground truth spectra from the Wells, Nevada sequence. Tomographic efforts in Asia rely on collections of temporary networks and permanent stations, and preparation includes noise analysis for undocumented instrument changes, relative calibration of channels and array elements, and data culling using manual and automated methods. Network based Pg/Lg discriminants have confirmed earlier results showing that 2-D path calibration improves performance in intermediate bands (2-6 Hz), thus improves discrimination coverage. We applied relative coda methods to Asia sequences to obtain GT spectra. The method generalizes spectral ratio techniques by converting collections of high precision, pairwise relative coda measurements to absolute spectra assuming an omega-2 source model, allowing simultaneous analysis of large numbers of events. Apparent stress results vary significantly for smaller events, and for the Wenchuan sequence, is more heterogeneous over the southern, thrusting segment of the slip plane. The ground truth spectra were used to constrain a joint inversion for frequency dependent attenuation and site terms of the four regional phases, as well as moment and corner frequency of each event. Absolute calibration based on high quality spectral ground truth will allow the examination of test site biases on regional phase and coda amplitudes, and lead to transportable yield estimation techniques. Models may be validated using the spectral ground truth in leave-one-out studies, as is done for traveltime models.

OBJECTIVES

We seek models that will allow the prediction of absolute spectral levels, for purposes of event identification and yield estimation. Models can be constrained and validated using spectral ground truth, obtained using relative coda techniques, with overall levels set by regional moment tensor studies. Spectral ground truth is used to break source-path (corner frequency-Q) tradeoffs, allowing extension of models into poorly covered regions, and can be used for model validation. Models will allow the isolation of near-source effects on explosion spectra, and the evaluation of test site biases, thus enable transportable, regional phase yield estimation.

RESEARCH ACCOMPLISHED

Spectral Ground Truth

Absolute spectral levels can be obtained for event clusters using spectral ratios of coda waves (Mayeda et al., 2007), and direct regional phases (Fisk and Taylor, 2007). These authors show that ratios eliminate common path and site effects, leading to a well-posed inversion for relative moment and corner frequencies. Independently determined moments of one or more cluster events allow absolute levels to be fixed.

We have developed a technique that extends the high precision, relative coda method of Mayeda et al., (2007) to include large numbers of events. Coda amplitudes are compared directly for all event pairs within a preset distance from each other. Minor adjustments are made for differing distance to the station using known variations in envelope peak time, coda shape, and path. Amplitude ($\log_{10}$) differences are stacked for various stations and channels, for each pair, then inverted to determine relative spectral levels for each band, to which we fit moment and corner frequency for each event, as well as a frequency dependent transfer function.

In an initial test, we applied the technique to study source-spectral parameters of over 1000 aftershocks of the Great Wenchuan Earthquake of May 12, 2008 (Figure 1). For this test, we processed envelopes in narrow bands between 0.03 and 8 Hz and used an inter-event cutoff of 50 km for frequencies above 0.5 Hz, increasing to 300 km for the lowest band. CMT scalar moments for many of the larger events were used to set the absolute level. Results show that apparent stress ranged from 0.1 to 10 MPa, and was slightly higher for larger aftershocks (Figure 2). This observation supports conclusions of Mayeda et al., (2007) concerning a break in scaling behavior at magnitude 5.5 or so. Higher stresses for large events are hypothesized by these authors as representing the regional stress state, while the scatter in stress for smaller events, including many low stress events, reflects spatial fluctuation of stress in the source region following the main shock. Envelopes for similar sized, nearby events with greatly differing stress levels show that the scatter is a real effect (Figure 3). Spectra from these events could be used to constrain absolute levels for events throughout this region. In this study, we will use source parameters of the larger Wenchuan events, excluding the mainshock, as well as those from other Asia clusters to constrain multi-band, multi-phase amplitude tomography for 2-D attenuation, site terms, and source parameters.

Amplitude Tomography using Spectral Ground Truth Constraints

Attenuation models are critical for magnitude and yield work (e.g., Nuttli, 1973) and benefit event identification studies through the reduction of discriminant scatter for distributions of earthquakes across large areas. Phillips et al. (1998) showed that 2-D empirical path correction for 0.5-8 Hz Pn, Pg, Sn and Lg phases reduced discriminant scatter in earthquake populations in China, especially for lower and intermediate bands (0.5-6 Hz). The effect in intermediate bands (2-6 Hz) is of particular importance as discrimination performance degrades toward low frequency (Walter et al., 1995; Taylor 1996). Discrimination is known to perform well in high bands (> 6 Hz), but signal-to-noise considerations limit the range at which those bands are observed. Thus, intermediate band discrimination is of importance in extending discrimination to smaller events and larger distances.

Tomographic models are superior to empirical models as attenuation can be constrained in areas without reference events, but that are crossed by raypaths from outside events. The Los Alamos team has been active in producing such models using a wide range of techniques (Phillips et al., 2000, 2005, 2008; Phillips and Stead, 2008), including dual-phase tomography (Phillips et al., 2001), Bayesian approaches (Taylor et al., 2003), accounting for left censored amplitude data (Taylor et al., 2003), and spherical earth spreading models for Pn (Yang et al., 2007). This has and continues to be an active area of research in the community (e.g., Campillo, 1987; Jin and Aki, 1988; Xie et al., 2006; Mitchell et al., 1997; Pei et al., 2006; Mayeda et al., 2005; Ford et al., 2009; Pasyanos et al., 2009).

Here, we describe a tomography scheme that jointly inverts amplitude data for multi-phase, multi-band attenuation, site and source terms, based on the MDAC formulation (Walter and Taylor, 2002). The critical component in the

inversion is to break the tradeoff between source and attenuation using constraints from the ground truth spectra described above. Additional absolute level constraints are applied through collections of regional moments in the area. Absolute levels will be added to the site terms, which become the absolute site terms described by Malagnini et al., (2006). We perform this inversion in two ways: 1) inversion for 2-D Qo and η ($Q=Qo\ f^{\eta}$; f, frequency) and frequency dependent absolute site terms for all phases, and moment and apparent stress (or corner frequency) for each event, and 2) 2-D Q and site terms for all bands and phases, moment and apparent stress for all events. Inversion 1 is the most restrictive as attenuation and source terms are explicit functions of frequency; however, experience with USArray amplitudes has shown us that the restrictions are not particularly harmful in terms of fit to data.

We apply these inversions to a data set of nearly 1.7 million east, central and south Asia Pn, Pg, Sn, and Lg amplitudes, for 12 bands between 0.5 and 10 Hz. We use 979 stations, many from IRIS and PASSCAL collections, and just over 10,000 continental events selected in geographic bins based on catalog quality, including ground truth (GT<=25) events culled from catalog data, magnitude, and coverage. Amplitudes are windowed using picks and predicted arrivals. When first P picks and predictions differ, that time shift is applied to predicted onsets for other phases.

We limit amplitudes to intervals of consistent noise level to avoid contamination by undocumented response changes. Amplitudes are further limited to be within an order of magnitude of fits to regionally varying 1-D models to avoid noise and coda measurements at distance (e.g. Phillips et al., 2008). Relative amplitudes for various channels and array elements are then quantified using common events, and those measurements are combined prior to inversion. A 3-sigma trim is applied to residuals of initial, smooth tomography models to cull remaining outliers.

We show 2-D Qo and η from Inversion 1 in Figures 4-5. The Qo results are similar to 1-Hz results from single-phase inversions presented at past reviews. Frequency dependence terms η are not inversely correlated with Qo. We observed inverse correlation for similar studies of USArray data, with low Qo associated with higher η, and vice versa. Frequency dependence for Pn Q is low, perhaps resulting from the frequency dependent Yang et al. (2007) spreading model used for that phase. Source parameters show typical scaling (Figure 7) with a weak tendency towards scaling that is steeper than self-similar. Pn residuals are highest (Figure 8), followed by Pg, Sn, and Lg. Pn windows are short in this study (8.1 – 7.6 km/s), which may partially explain their higher residuals. Residuals for Inversion 2 are not shown, but they are slightly higher than those depicted. The reason for this is simply that regularization parameters were chosen too large for the latter runs, and no scientific significance is attached to the difference. Figures 8 and 9 show results of a checkerboard test using perfect data. This demonstrates code fidelity and upper limits of spatial resolution with this data set. Synthetic source parameters and site terms were also recovered well.

CONCLUSIONS AND RECOMMENDATIONS

Ground truth spectra can be used in to constrain multi-band, multi-phase amplitude tomography to produce models that predict absolute spectra from regional phase earthquake amplitudes. Further, spectral ground truth can be used to validate propagation models in the same way that location ground truth is used to validate traveltime models. Such models are critical for regional phase magnitude, yield and event identification analyses. Collection of spectral ground truth must be a collaborative effort over time by the community, as has been the case for location ground truth.

ACKNOWLEDGEMENTS

This study relied on IRIS and PASSCAL waveform collections, and we greatly appreciate help from IRIS DMC personnel. Graphics were made with GMT software. Valuable discussions with M. Fisk are acknowledged.

REFERENCES

Campillo, M. (1987). Lg wave propagation in a laterally varying crust and the distribution of the apparent quality factor in central France, *J. Geophys. Res.* 92: 12,604–12,614.

Fisk, M. and S. R. Taylor, (2007). Robust magnitude and path corrections for regional seismic phases in Eurasia by constrained inversion and enhanced kriging techniques, in *Proceedings of the 29th Monitoring Research Review: Ground-Based Nuclear Explosion Monitoring Technologies*, LA-UR-07-5613, Vol. 1, pp. 24–33.

Ford, S.R., W.S. Phillips, W.R. Walter, M.E. Pasyanos, K.M. Mayeda, and D.S. Dreger (2009). Attenuation tomography of the Yellow Sea/Korean Peninsula from coda-source normalized and direct Lg amplitudes, *Pure Appl. Geophys*., doi:10.1007/s00024-009-0023-2.

Jin, A., and K. Aki (1988). Spatial and temporal correlation between coda-Q and seismicity in China, *Bull. Seismol. Soc. Am*. 78: 741–769.

Malagnini, L., P. Bodin, K. Mayeda, A. Akinci (2006). Unbiased moment-rate spectra and absolute site effects in the Kachachh Basin, India, from the analysis of the aftershocks of the 2001 Mw 7.6 Bhuj earthquake, *Bull. Seismol. Soc. Am.* 96: doi:10.1785/0120050089.

Mayeda, K.M., L. Malagnini, W.S. Phillips, W. Walter, and D. Dreger, (2005). 2-D or not 2-D, that is the question: A northern California test, *Geophys. Res. Lett.* 32: L12301, doi:10.1029/2005GL022882.

Mayeda, K., L. Malagnini, W. R. Walter, (2007). A new spectral ratio method using narrow band coda envelopes: Evidence for non-self-similarity in the Hector Mine sequence, *Geophys. Res. Lett.*, doi:10.1029/2007GL030041.

Mitchell, B. J., Y. Pan, J. Xu, and L. Cong (1997). Lg coda Q variation across Eurasia and its relation to crustal evolution, *J. Geophys. Res*. 102: 11767–22779.

Nuttli O. W. (1973). Seismic wave attenuation and magnitude relations for eastern North America, *J. Geophys. Res.* 78: 876–885.

Pasyanos, M.E., W.R. Walter, and E.M. Matzel (2009). A simultaneous multiphase approach to determine P-wave and S-wave attenuation of the crust and upper mantle, *Bull. Seismol. Soc. Am*. 99: 3314–3325.

Pei, S., J. Zhao, C. A. Rowe, S. Wang, T. M. Hearn, Z. Xu, H. Liu, and Y. Sun (2006). M_L amplitude tomography in North China, *Bull. Seismol. Soc. Am.* 96: 1560–1566, doi: 10.1785/0120060021.

Phillips, W. S., G. E. Randall and S. R. Taylor (1998). Path correction using interpolated amplitude residuals: An example from central China, *Geophys. Res. Lett*. 25: 2729–2732.

Phillips, W. S., H. E. Hartse, S. R. Taylor, and G. E. Randall (2000a). 1 Hz Lg Q Tomography in central Asia, *Geophys. Res. Lett*. 27: 3425–3428.

Phillips, W. S., H. E. Hartse, S. R. Taylor, A. A. Velasco, and G.E. Randall (2001). Application of regional phase amplitude tomography to seismic verification, *PAGEOPH*, 158**:** 1189–1206.

Phillips, W. S., H. E. Hartse, and J. T. Rutledge (2005). Amplitude ratio tomography for regional phase Q, *Geophys. Res. Lett*. 32: doi:10.1029/2005GL023870.

Phillips, W. S. and R. J. Stead (2008). Attenuation of Lg in the western US using the USArray, *Geophys. Res. Lett*. 35: L07307, doi:10.1029/2007GL032926.

Phillips, W. S., R. J. Stead, G. E. Randall, H. E. Hartse, and K. Mayeda (2008). Source effects from broad area network calibration of regional distance coda waves, in Advances in Geophysics, 50, *Scattering of Short Period Waves in the Heterogeneous Earth*, H. Sato and M.C. Fehler, Eds., 319–351.

Taylor, S. R. (1996). Analysis of high frequency Pg/Lg ratios from NTS explosions and western US earthquakes, *Bull. Seismol. Soc. Am*. 86: 1042–1053.

Taylor, S. R., X. Yang, and W. S. Phillips (2003). Bayesian Lg attenuation tomography applied to eastern Asia, *Bull. Seismol. Soc. Am*. 93: 795–803.

Walter, W.R., K.M. Mayeda, and H.J. Patton, (1995). Phase and spectral ratio discrimination between NTS earthquakes and explosions: 1. Empirical observations, *Bull. Seismol. Soc. Am.* 85: 1050–1067.

Walter, W. R. and S. R. Taylor (2002). A revised magnitude and distance amplitude correction (MDAC2) procedure for regional seismic discriminants: theory and testing at NTS, Lawrence Livermore National Laboratory, UCRL-ID-146882, pp. 13.

Yang, X., T. Lay, X.-B. Xie, and M. S. Thorne (2007). Geometric spreading of Pn and Sn in a spherical Earth model, *Bull. Seism. Soc. Am.* 97: 6, 2053-2065.

Xie, J. K., Z. Wu, R. Liu, D. Schaff, Y. Liu, and J. Liang (2006). Tomographic regionalization of crustal Lg Q in eastern Eurasia, *Geophys. Res. Lett*. 33: L03315, doi:10.1029/2005GL024410.

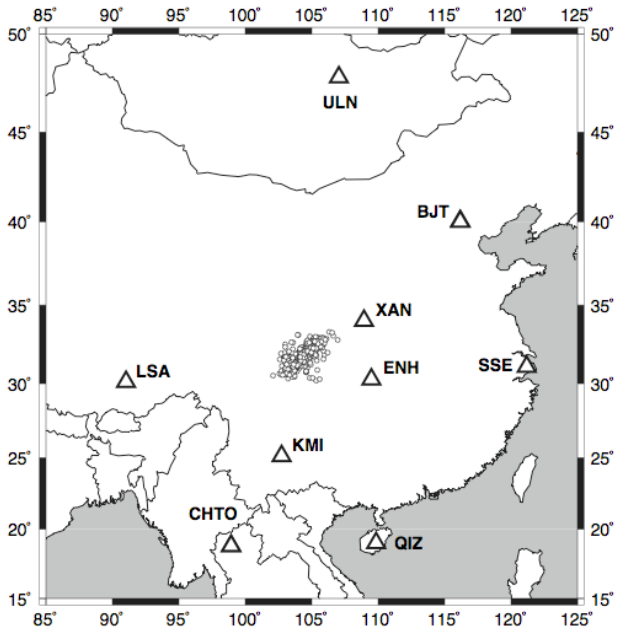

Figure 1. Stations (triangles) and events (EDR bulletin, circles) used in the relative coda source study of Wenchuan aftershocks.

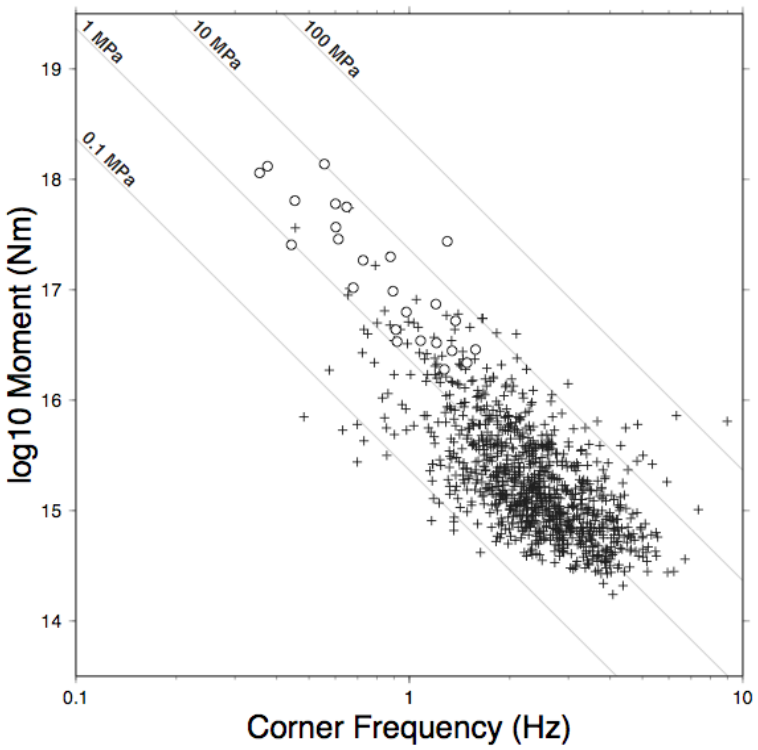

Figure 2. Moments and corner frequencies obtained for Wenchuan aftershocks using the relative coda technique. Open circles represent events for which CMT moments were used as constraints, crosses represent the remainder. Diagonal lines represent apparent stress, as noted.

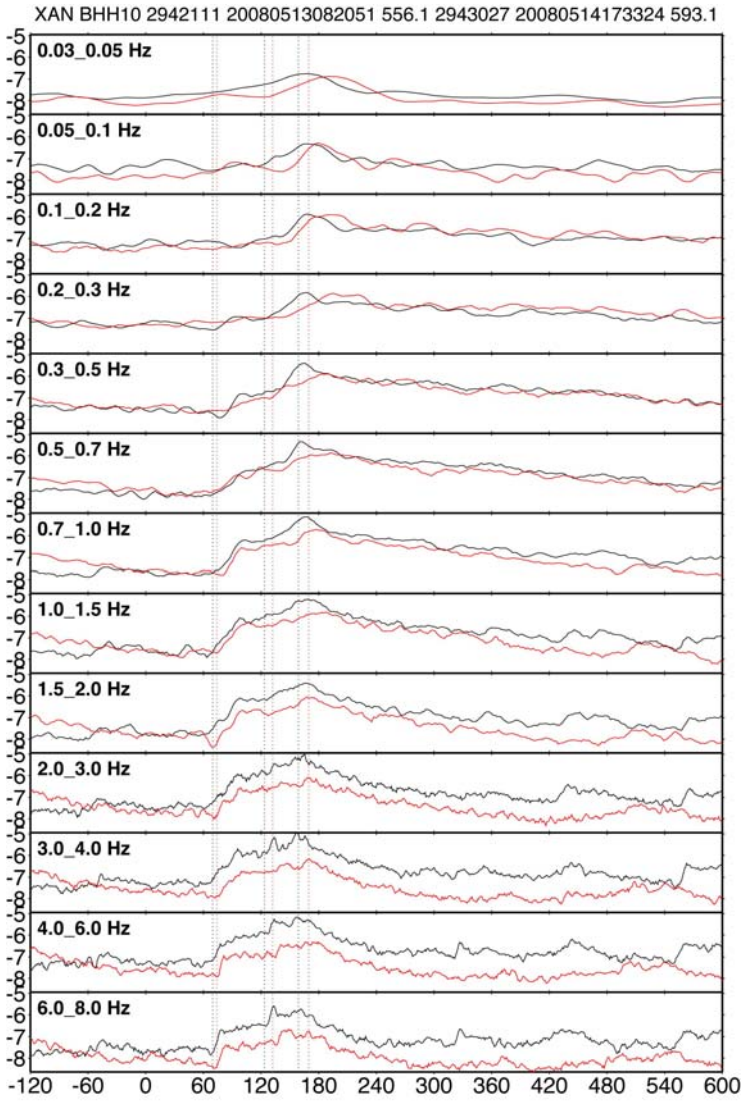

Figure 3. Envelopes for nearby, similar-sized Wenchuan events of differing stress for station XAN (Xian). Predicted P, Sn, and Lg peak envelopes are marked for both events. Band limits are noted. Time is seconds from the origin, envelope units are m/s.

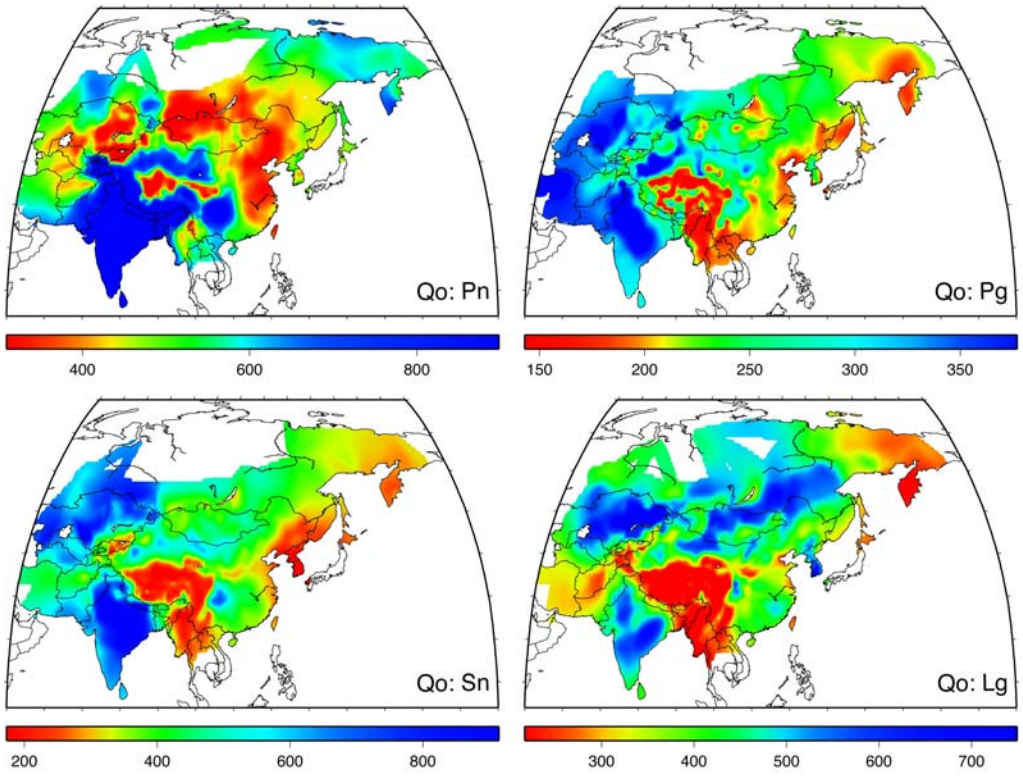

Figure 4. Q at 1 Hz (Qo) for regional phases in central, south and east Asia. Results were obtained using the Yang et al (2007) spreading for Pn, power law spreading of 0.7 for Pg, 1.1 for Sn, and 0.5 for Lg.

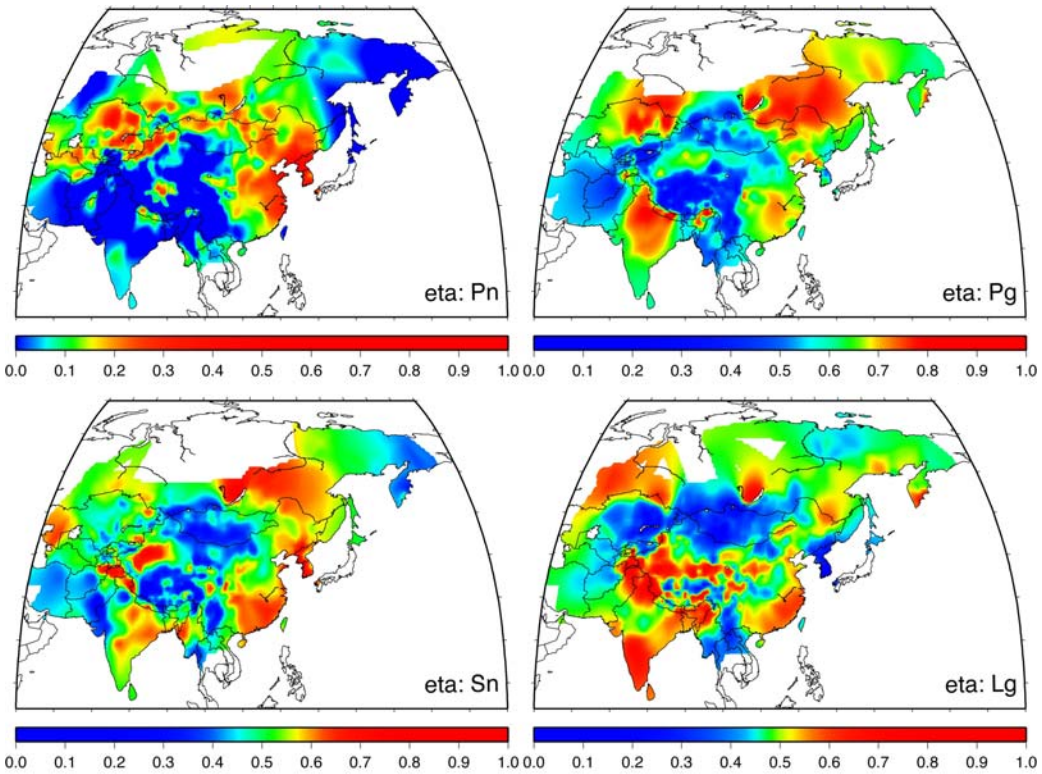

Figure 5. Frequency dependence of Q (η) for regional phases

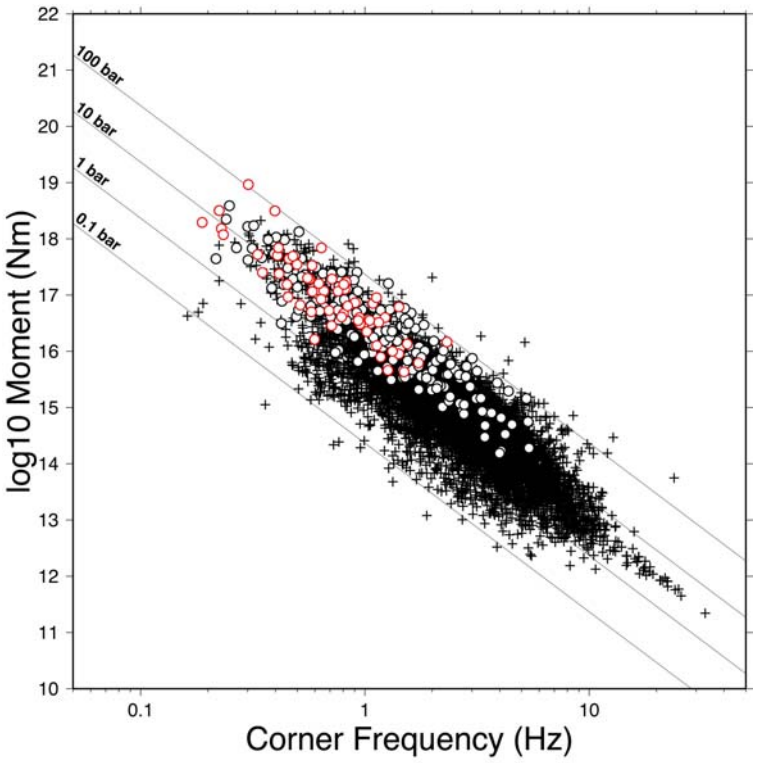

Figure 6. Moment and corner frequency for events used in the inversion. Apparent stress is noted (1 bar = 0.1 MPa). Black circles represent events with scalar moments that were used as constraints. Red circles represent events with ground truth spectra from relative coda studies that were used as constraints. The convergence towards 3 bars for small events is the result of regularizing the inversion to favor self-similar scaling with average stress when corner frequencies cannot be constrained.

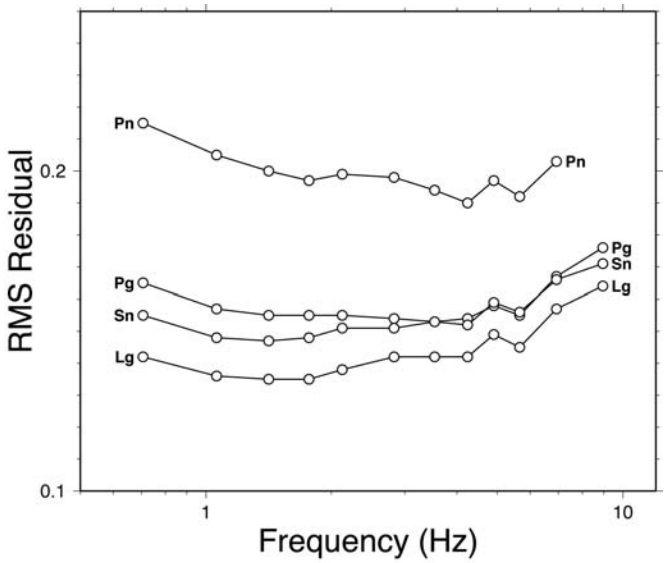

Figure 7. Inversion residuals by band corresponding to results shown in Figures 4-6, for phases as annotated.

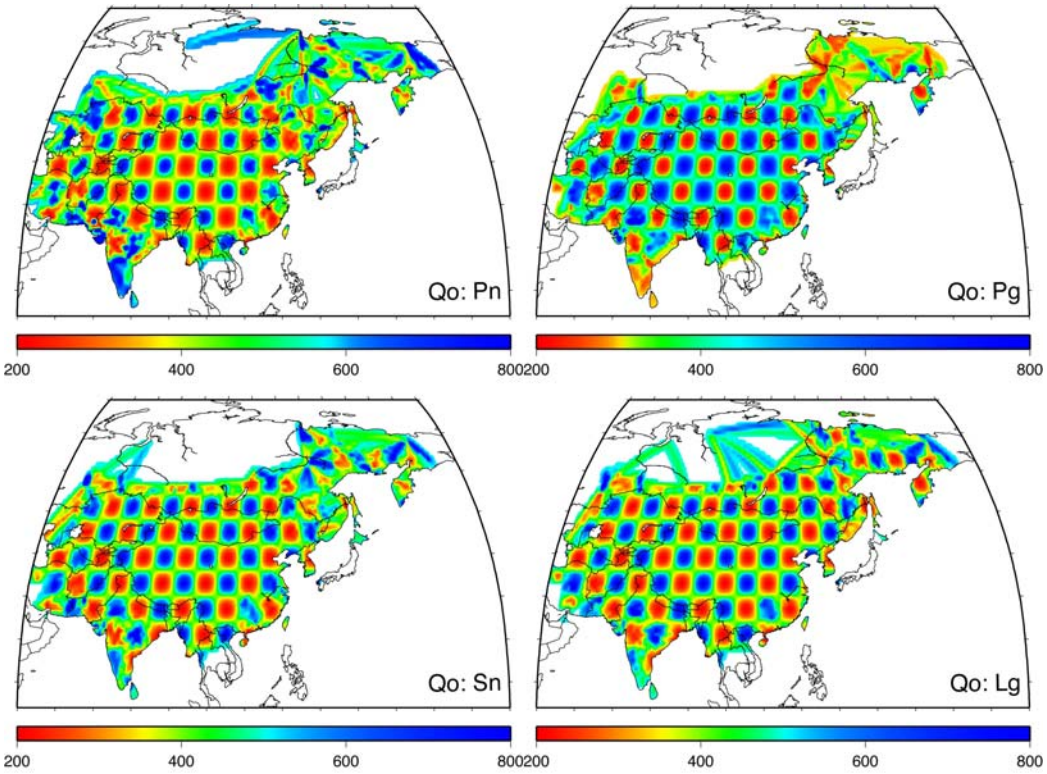

Figure 8. Q at 1 Hz (Qo) for synthetic data test, 5 degree sine model, Q 200 to 800, η 0.3-0.7.

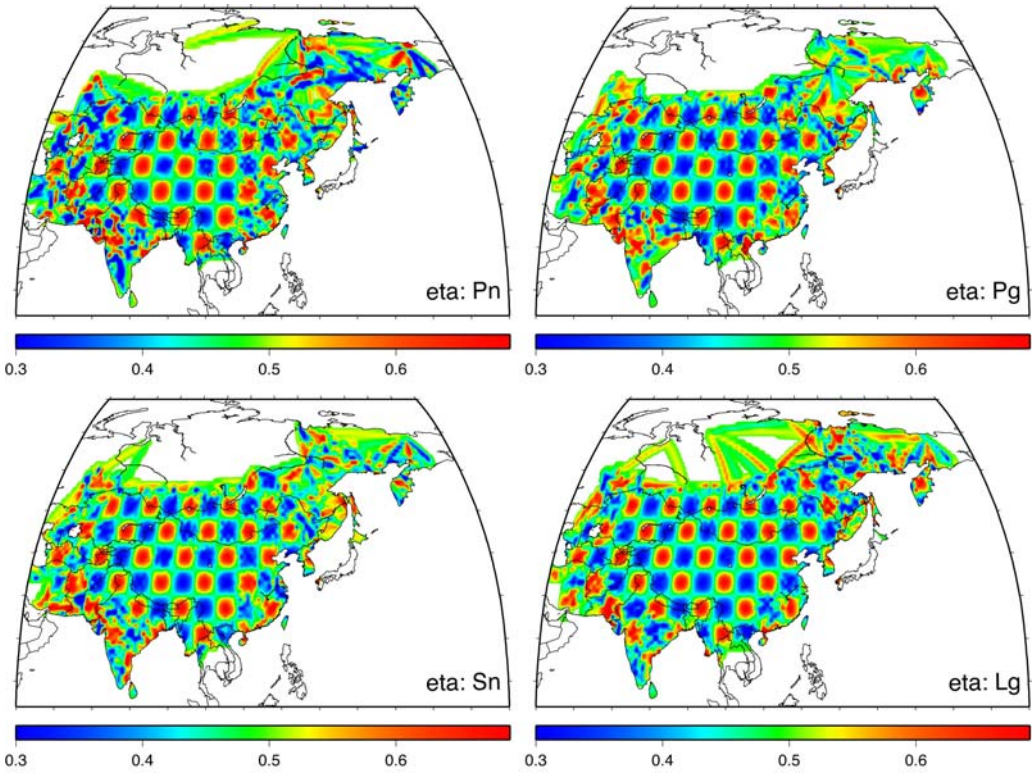

Figure 9. Frequency dependence of Q (η) for synthetic data test as described above.